

# Antennas on CubeSat Platforms: Accurate RF Predictions

C. Cappellin<sup>(1)</sup>, M. M. Bilgic<sup>(1)</sup>, J. R. de Lasson<sup>(1)</sup>, O. Borries<sup>(1)</sup>

<sup>1</sup> TICRA: Copenhagen, Denmark, {cc; mmb; jrld; ob}@ticra.com

**Abstract**— A typical 3U and 6U CubeSat hosting antennas ranging from the low UHF to the higher Ka band are modelled in the ESTEAM software package. The antennas are inspired by recent designs published in the literature. RF performances of the antennas installed on the CubeSats are computed with the MoM/MLFMM full wave analysis method and compared with the ones in the absence of the CubeSat platform. The results show that the RF performances of the antennas are substantially changed once these are installed on the CubeSats, indicating that platform scattering and coupling with the neighboring antennas must be included and accounted for already in the antenna design phase.

**Index Terms**—CubeSats, platform scattering, full wave analysis, installed RF performances.

## I. INTRODUCTION

CubeSats made of one or multiple 10 cm X 10 cm X 10 cm units, the so-called 1 U, are the smallest satellites in the market. Their use started around twenty years ago, pushed by universities which used them as educational tools and low-cost technology demonstration platforms. Today, CubeSats, especially in their 3U, 6U and 12U versions, attract the attention of investors and satellite manufacturers for two main reasons. Firstly, since they allow constellations of small satellites in LEO orbit, which are the alternative for telecommunication applications to traditional large satellites in GEO orbit, referred to as old space, [1]. Secondly, since the low cost and short development time of designing and launching a CubeSat make space research more accessible and open up for new applications and services, referred to as new space, as demonstrated, for example, by some of the recent achievements of NASA JPL [2]-[3].

CubeSat antennas realize functions like those of traditional large satellite antennas, i.e., TT&C, payload data downlink and GNSS reception [4]. With CubeSat missions operating from 400 MHz (UHF band) up to 110 GHz (W band), antennas ranging from miniaturized patches to deployable reflectors and reflectarrays have been designed and, in most cases, manufactured. Wideband or dual band elements are also currently under study to reduce the total number of required antennas.

The RF requirements that CubeSats antennas shall comply with become more challenging as the missions evolve in complexity. Moreover, the proximity of the antennas on a 3U and 6U CubeSat makes the coupling between the antennas and the CubeSat body stronger than on traditional large satellites. Such a coupling must therefore be

included already in the antenna design phase [5]-[6]. Accurate and fast full wave simulations are thus necessary in the new space market to design antennas that can meet the pattern, impedance matching and bandwidth requirements, once installed on the CubeSat. Despite its importance, platform scattering on CubeSats is not a standard task during the CubeSat development. Moreover, it is not clear if the software tools used in the old space satisfy the needs of the new space as well.

The TICRA Tools suite, including GRASP, ESTEAM, CHAMP 3D and soon QUPES, is the tool of choice for antenna design and analysis in the old space sector. In particular, the ESTEAM software product, with its higher-order Method of Moments (MoM) algorithm accelerated by the MLFMM solver, is well suited for the RF design of general antennas and is considered the industry standard for platform scattering [7]-[8].

The purpose of the present paper is to evaluate if the higher-order MoM/MLFMM solver used in the old space can accurately model the antennas of the new space, and to investigate if platform scattering is an issue in CubeSats. This will be done by modelling two CubeSat satellites that were recently launched. In particular, Section II describes the full wave RF modelling of a 3U CubeSat hosting 4 UHF dipoles, a patch antenna and a helix antenna. Section III focuses on the full wave modelling of a 6U CubeSat hosting a reflector antenna, a patch antenna and solar panels. Conclusions are finally drawn in Section IV.

## II. 3U CUBESAT MODEL

The 3U CubeSat modelled in this work is inspired by the GOMX-3 satellite, developed by GomSpace and ESA and launched in 2015 [9]. The purpose of the satellite was to demonstrate reception of aircraft ADS-B (Automatic Dependent Surveillance-Broadcast) signals and measurement of the signal quality of geostationary telecommunication satellites in L band.

GOMX-3 hosted five antennas, see Fig. 1: A deployable helix antenna to measure the ADS-B signals, four UHF monopoles to establish communication in the initial stages after deployment, a Global Positioning System (GPS) antenna to keep track of the satellite orbit, an L band antenna to measure the quality of service supplied by the L band GEO communication satellites, and an X band transmitter patch antenna. All antennas operate in circular polarization,

the first four were designed by GomSpace, while the X band patch was developed by Syrlinks. The helix and the UHF antennas were based on designs used in previous missions, while the L band, X band and GPS antennas were developed specifically for GOMX-3.

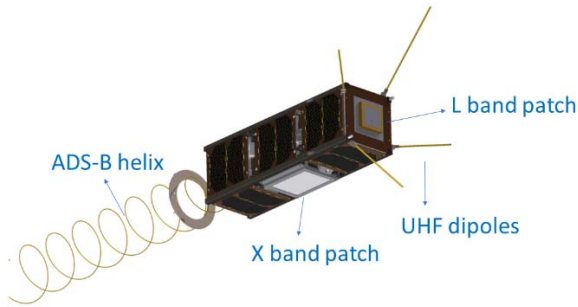


Fig. 1. GOMX-3 satellite from GomSpace. The GPS antenna is on the lateral face and not clearly visible in this picture.

The L band patch antenna designed by GomSpace is visible on the left side of Fig. 2, located on the 10 cm x 10 cm face of the satellite. The patch works in the [1.525:1.565] GHz band and is located on a high dielectric substrate with high permittivity, in order to reduce the side length of the patch to 36 mm. The excitation is through a coaxial cable. A slot in the centre and corner truncations in the patch rim generate circular polarization with axial ratio of less than 6 dB. The cut-outs on the side edges of the patch increase the impedance bandwidth, and allow a RL of around 15 dB and a gain of around 5.5 dB in the desired frequency band [8].

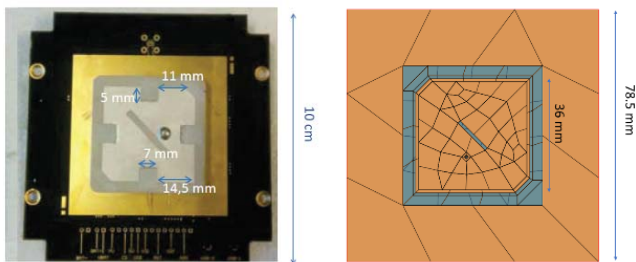


Fig. 2. L band patch antenna: On the left the antenna designed and manufactured by GomSpace for GOMX-3 [9], and on the right the antenna designed and modelled by TICRA for the present work.

The L band patch antenna modelled by TICRA in this work is shown on the right side of Fig. 2. The patch has the same size length of 36 mm and uses a dielectric with permittivity equal to 7. The antenna is modelled in the TICRA’s ESTEAM product: The radiation pattern for the bare antenna (that is, in the absence of the CubeSat platform) is seen in Fig. 3. Due to the missing cut-outs in the patch rim, the band is slightly narrower: A RL of around 14 dB is achieved in the [1.525:1.555] GHz band. The axial ratio (AR) is 4 dB. As seen in Fig. 1, the patch antenna is located on the top face of the 3U CubeSat, in between the four UHF dipoles. It is therefore interesting to compute the interaction between the patch and the dipoles, and to investigate how this affects the patch antenna pattern. The top face and the UHF dipoles are modelled in ESTEAM as a CAD file. A

plot of the currents induced on the patch, dipoles and top face, when the patch is radiating and the dipoles are matched, is seen in Fig. 4. The corresponding radiation pattern is shown in Fig. 5.

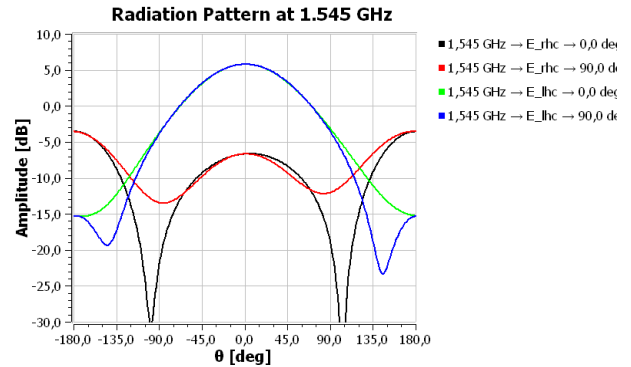


Fig. 3. Radiation pattern at 1.545 GHz of the bare L band patch antenna from TICRA.

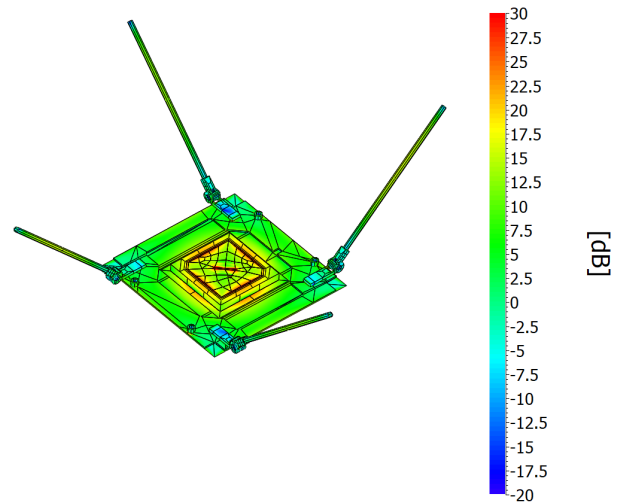


Fig. 4. Amplitude of the total electrical currents induced on the top face of the 3U CubeSat, when the L band patch is radiating and the UHF dipoles are matched.

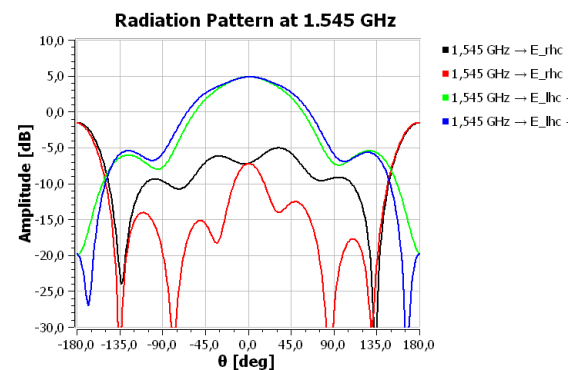


Fig. 5. Radiation pattern at 1.545 GHz of the L band patch antenna from TICRA in presence of the matched UHF dipoles and top face.

When comparing Fig. 3 with Fig. 5 it is seen that the effect of the dipoles and the top face on the patch antenna pattern is significant. In particular, the peak drops by 0.9 dB

and the back lobe changes shape. The cross-polar component remains at the same level but changes form and the AR deteriorates by 1 dB compared to the performances of the bare patch antenna. The RL of the patch antenna is around 19 dB and thus it is not negatively affected by the dipoles. The other scattering parameters with the UHF ports are below -50 dB, indicating that the UHF and L band ports are not coupled.

A helix antenna similar to the one on GOMX-3 is finally added to the 3U CubeSat model. The helix antenna is modelled in ESTEAM as a curved wire excited by a voltage generator. The helix has a diameter of 8.5 cm, a pitch angle of 8° and 6.5 turns, and works at 1.090 GHz.

The pattern of the patch antenna in presence of the matched UHF dipoles, the full 3U CubeSat platform and the helix antenna is seen in Fig. 7, as dotted lines, while the solid lines are those from Fig. 5. The induced currents are shown in Fig. 6. Changes are visible in the main beam for both the co-polar and the cross-polar components. It is thus concluded that the UHF dipoles, the full 3U CubeSat and the helix antenna influence the pattern of the L band patch antenna, when the patch antenna is radiating.

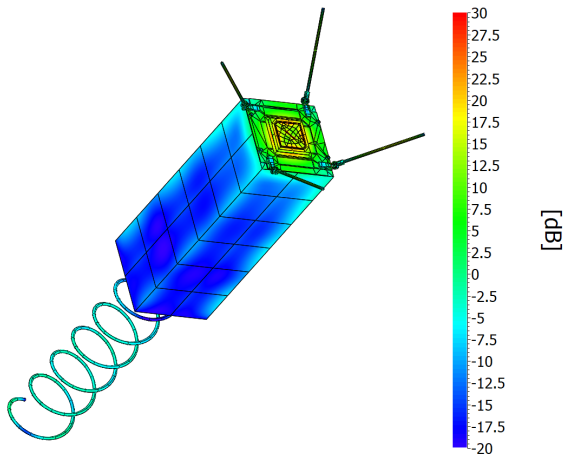


Fig. 6. Full wave model of the 3U CubeSat with the ADS-B helix antenna, four UHF dipoles and the L band patch used for the platform scattering analysis of Section II.

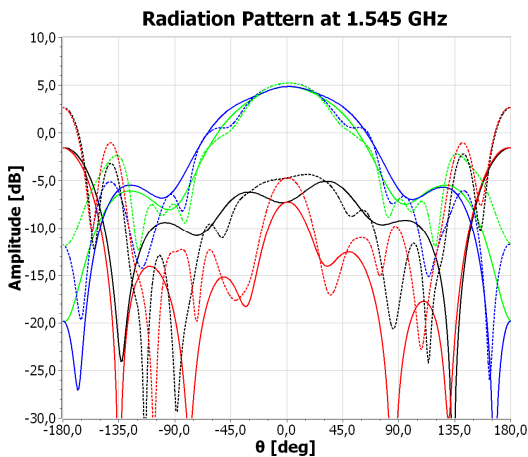


Fig. 7. Radiation pattern at 1.545 GHz of the L band patch antenna from TICRA in presence of the matched UHF dipoles (solid, same as in Fig. 5), and the helix and the full 3U CubeSat (dashed).

### III. 6U CUBESAT MODEL

The 6U CubeSat modelled in this work is inspired by the RainCube mission, developed by NASA JPL and launched in 2018 [3]. RainCube had the purpose to develop, launch and operate the first radar instrument on a 6U CubeSat. The instrument was made by a lightweight deployable reflector antenna with a 500 mm projected aperture working at 35.75 GHz. The spacecraft is displayed in Fig. 8.

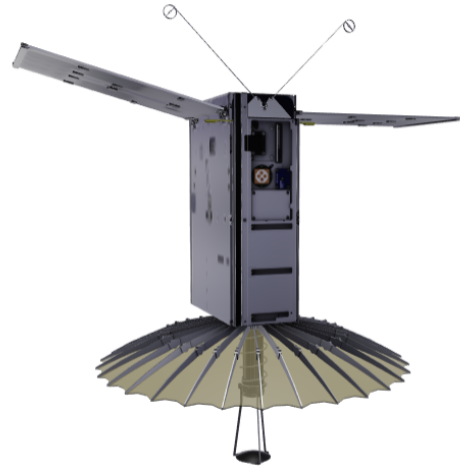


Fig. 8. The RainCube spacecraft, as available at [10].

The reflector antenna modelled by TICRA is a Cassegrain ring focus working at 33 GHz in linear polarization and designed with CHAMP 3D. The main reflector has a diameter of 500 mm and a focal length of 220 mm, while the subreflector has a diameter of 60 mm. The input waveguide radius is 3.3 mm, which ensures TE<sub>11</sub> mode propagation in the 32-34 GHz band. A waveguide step and one conical section are added to the input waveguide, to achieve a RL of 15 dB, as shown in Fig. 9. The subreflector has a thickness of 5 mm and is supported by three circular struts. Finally, 30 ribs are added with GRASP to model the pillowing effect of the deployable reflector. The MoM/MLFMM solver of ESTEAM is finally used to compute the pattern of the antenna, with the associated MoM mesh shown in Fig. 10. The reflector is assumed perfect electric conducting.

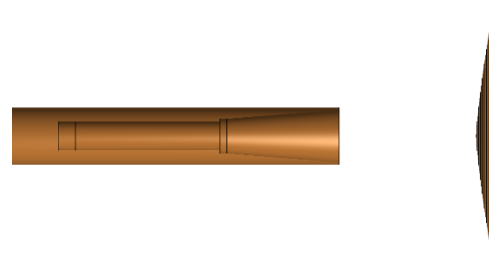


Fig. 9. Details of the waveguide illuminating the subreflector.

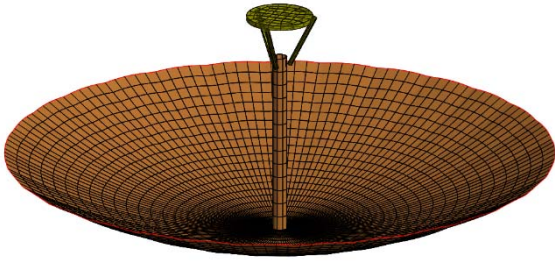


Fig. 10. MoM mesh of the reflector antenna considered for the 6U CubeSat model of this work.

The pattern of the bare reflector antenna in free space is seen in Fig. 11. Adding solar panels and the full 6U platform in the full wave analysis, see Fig. 12, does not affect the pattern of the reflector antenna, since the CubeSat and most of the solar panels are shadowed by the reflector surface.

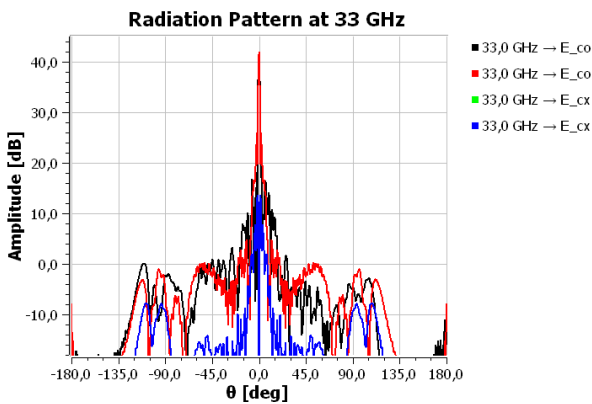


Fig. 11. Radiation pattern at 33 GHz of the bare reflector antenna of Fig. 10.

On the lateral side of the RainCube platform there is an S band patch antenna for ground communication and data downlink, as shown in Fig. 12. The antenna model developed by TICRA for this work is shown in Fig. 13. The patch is squared, with a side length of 37.3 mm. It is located on a dielectric of 2.72 mm height with permittivity equal to 3, on a ground plane of 63.6 mm. A coaxial port excites the antenna in linear polarization. The pattern of the bare S band patch is shown in Fig. 14, as computed with ESTEAM.

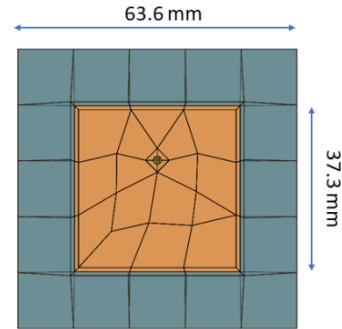


Fig. 13. S band patch antenna modelled by TICRA for this work.

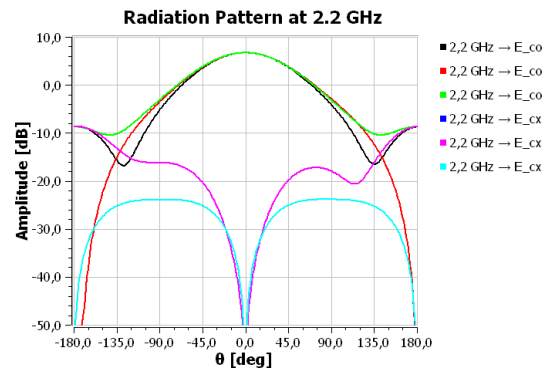


Fig. 14. Radiation pattern at 2.2 GHz of the bare patch antenna of Fig. 13.

The pattern of the S band patch located on the side of the 6U platform in presence of one solar panel is shown in Fig. 15. When comparing Fig. 14 with Fig. 15 it is possible to see that the co- and cross-polar pattern is strongly affected by the solar panel and satellite face, especially in the  $\phi=0^\circ$  deg plane, which is the plane given by the two structures. The corresponding induced currents are shown in Fig. 16.

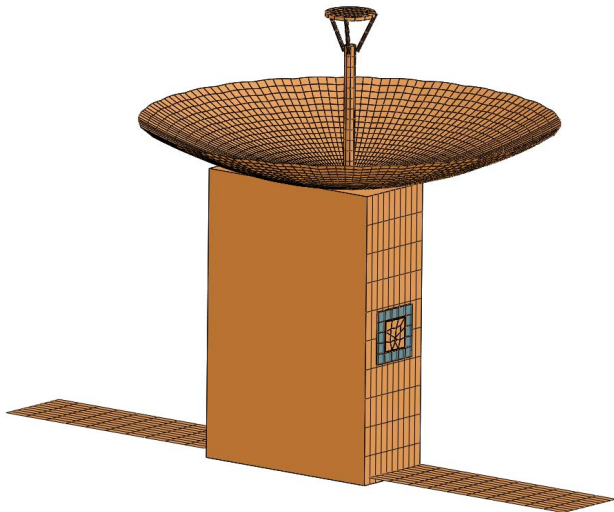


Fig. 12. 6U CubeSat model in TICRA Tools showing the reflector antenna, the 6U CubeSat, the S band patch antenna and the solar panels considered in this paper.

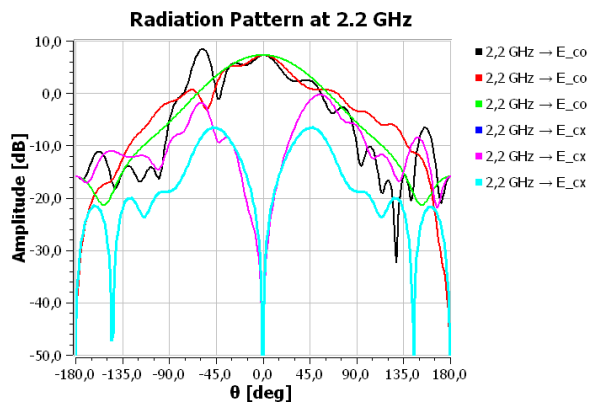


Fig. 15. Radiation pattern at 2.2 GHz of the patch antenna of Fig. 13 located on the lateral side of the 6U platform and in presence of the solar panel.

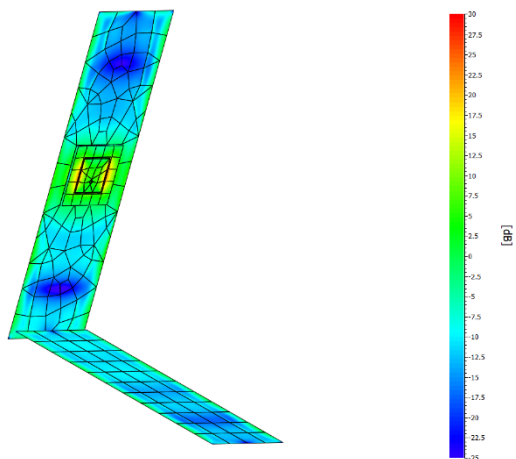


Fig. 16. Amplitude of the total electrical currents induced on the lateral face of the 6U satellite and one solar panel, when the S band patch is radiating.

#### IV. CONCLUSIONS

A 3U CubeSat, inspired by the GOMX-3 satellite of GomSpace and ESA, and a 6U CubeSat, inspired by the RainCube satellite of NASA JPL, were modelled with the higher order full wave solver of the ESTEAM software package from TICRA. On the 3U CubeSat a helix antenna working in the ADS-B band, four UHF dipoles and one L band patch antenna were considered. On the 6U CubeSat, a reflector antenna working at 33 GHz and a patch antenna working at 2.2 GHz were analysed.

The RF performances of the bare antennas and of the antennas installed on the CubeSats were computed. The results showed that the 3U CubeSat, the helix antenna and the UHF dipoles strongly influenced the pattern of the L band patch antenna, when the patch antenna was radiating, and the UHF dipoles were matched. On the 6U CubeSat, the lateral side of the satellite and the solar panel influenced the pattern of the S band patch antenna, while the pattern of the reflector antenna was not affected by them, due to the shadowing effect of the reflector.

The results show that the RF performances of the electrically small antennas are substantially changed once

installed on the CubeSats, indicating that platform scattering and coupling with the neighbouring antennas must be included and accounted for already in the antenna design phase. This work finally indicates that the higher-order full wave solver of the ESTEAM software may become an essential tool for the antenna designer working with next generation CubeSats.

#### REFERENCES

- [1] Y. Rahmat-Samii, V. Manohar, and J. M. Kovitz, "Think small, dream big: A review of recent antenna developments for CubeSats," *IEEE Antennas Propag. Mag.*, vol. PP, no. 99, pp. 1–1, 2017.
- [2] R. E. Hodges, N. Chahat, D. J. Hoppe, and J. D. Vacchione, "A deployable high-gain antenna bound for Mars: Developing a new folded panel reflectarray for the first CubeSat mission to Mars," *IEEE Antennas Propag. Mag.*, vol. 59, no. 2, pp. 39–49, April 2017.
- [3] N. Chahat, R. E. Hodges, J. Sauder, M. Thomson, E. Peral, Y. Rahmat-Samii, "CubeSat deployable Ka-band mesh reflector antenna development for Earth science missions," *IEEE Trans. Antennas Propag.*, vol. 64, Issue 6, June 2016.
- [4] S. Gao, et al., "Antennas for modern small satellites," *IEEE Antennas Propag. Mag.*, vol. 51, no. 4, 2009.
- [5] J. R. de Lasson, O. Borries, C. Cappellin, T. Rubæk, "High frequency Cubesat platform scattering using higher-order Method of Moments", *Proc. IEEE APS Symposium, San Diego, USA, July 2019.*
- [6] R. Fragnier, K. Elis, V. Laquerbe, R. Contreres, A. Bellion, B. Palacin, "Compact antennas for nano- and micro- satellites: development and future antenna needs at CNES", *Proc. 13<sup>th</sup> European Conference on Antennas and Propagation (EuCAP), Krakow, Poland, April 2019.*
- [7] E. Jørgensen, O. Borries, P. Meincke, M. Zhou, and N. Vesterdal, "New fast and robust modelling algorithms for electrically large antennas and platforms," *Proc. 9<sup>th</sup> European Conference on Antennas and Propagation (EuCAP), Lisbon, Portugal, April 2015.*
- [8] <https://www.ticra.com/software/esteam/>
- [9] A. Tatomirescu and G. F. Pedersen, J. Christiansen and D. Gerhardt, "Antenna system for Nano-satellite mission GOMX-3", *Proc. IEEE-APS Topical Conference on Antennas and Propagation in Wireless Communications (APWC), September 2016.*
- [10] <https://www.jpl.nasa.gov/cubesat/missions/raincube.php>